

# Single-Carrier Frequency-Domain Equalization for Orthogonal STBC over Frequency-Selective MIMO-PLC Channels

Mohsen Sheikh-Hosseini, Mohammad Molavi-Kakhki and Ghosheh Abed Hodtani  
Department of Electrical Engineering, Ferdowsi University of Mashhad, Mashhad, Iran  
mo\_sh240@stu.um.ac.ir, molavi@um.ac.ir, hodtani@um.ac.ir  
corresponding author: Mohsen Sheikh-Hosseini

**Abstract**—In this paper we propose a new space diversity scheme for broadband PLC systems using orthogonal space-time block coding (OSTBC) transmission combined with single-carrier frequency-domain equalization (SC-FDE). To apply this diversity technique to PLC channels, we first propose a new technique for combining SC-FDE with OSTBCs applicable to all dispersive multipath channels impaired by impulsive noise. The proposed technique is then applied to indoor and outdoor PLC channels under different channel scenarios in the presence of background and impulsive noises. We perform the simulations for SISO, MISO and MIMO configurations and show that a significant SNR gain is achieved when SC-FDE is combined with diversity techniques. We also compare our proposed technique with OFDM using Alamouti code for broadband PLC and show the superiority of our technique.

**Index Terms**—broadband power line communication, frequency-selective fading channel, impulsive noise, orthogonal space time block coding, single-carrier frequency-domain equalization.

## I. INTRODUCTION

Using power grid for communication purposes is not a new idea. In fact the use of narrowband power line communication (PLC) technology for management and monitoring of power networks started from early 1900s by using conventional single-carrier (SC) modulation in low frequency band (below 500kHz) supporting bit rates up to a few kbps. During the last decade, broadband low voltage PLC has received an increasing interest as an attractive solution for last mile access of communication networks, in-building networking and fast internet access. Recently with the emerging of smart grid concept, PLC technology has received great attention as a promising candidate for the smart grid where both narrowband and broadband PLC systems are proposed for smart grid applications like automatic meter reading, vehicle-to-grid communication and networking of consumer home appliances [1]-[2].

However, broadband communication over power lines requires a high bandwidth to support data rates in excess of 100Mbps and power lines are very harsh mediums for high speed transmission and impose serious limitations due to their time and frequency dependent attenuation and also due to impulsive noise and multipath effects [3]. The multipath nature of PLC channels is due to impedance mismatching of electrical networks where transmitted signal propagates along several paths with different attenuations and delays. Echo superposition of transmitted signal with different delays lead to inter-symbol interference (ISI) destroying transmitted data. High speed transmission in such time dispersive channels can span ISI over a remarkable number of data symbols. For example, in 100Mbps binary communication over typical PLC channel with 0.5-1.5  $\mu$ s delay spread, ISI span over 50-150 symbols [4].

Orthogonal frequency division multiplexing (OFDM) for its robustness to multipath echoes and selective fading is an attractive candidate for PLC systems and is adapted to some standards such as Homeplug1.0 and HomeplugAV. Despite its great attraction in academic and industrial communities, OFDM efficiency is limited by some drawbacks like high peak to average power ratio and carrier frequency offset sensitivity.

Single-carrier frequency-domain equalization (SC-FDE) is another technique for broadband communication over highly dispersive channels. Similar to OFDM, SC-FDE is a block transmission technique with cyclic prefix (CP) insertion at the transmitter, and using fast Fourier transform (FFT) and inverse FFT (IFFT) algorithms. The implementation complexity and achievable performance of SC-FDE is comparable to that of OFDM while avoiding the OFDM drawbacks [4]-[6]. Recent research activities in this area have focused on using STBCs combined with SC-FDE. For this combination the original symbol-level STBCs designed for flat channels have to be extended to block-level for frequency-selective channels. This was first proposed by Al-Dhahir for Alamouti code over a  $2 \times 1$  multi-input single-output (MISO) wireless channel [7]. However, this technique is only applicable to special structures of orthogonal STBC (OSTBC) where the elements of each time-slot are either from the set  $\{0, \pm x_1, \dots, \pm x_K\}$  or the set  $\{0, \pm \bar{x}_1, \dots, \pm \bar{x}_K\}$ , where  $\bar{x}_i$  is the complex conjugate of symbol  $x_i$ . An example of these codes is given in (A.1) in Appendix. This technique is not applicable to the OSTBCs in which the elements of time-slots are members of the set  $\{0, \pm x_1, \pm \bar{x}_1, \dots, \pm x_K, \pm \bar{x}_K\}$ . To overcome this limitation, we propose a new design method in section III.

For the first time, we addressed the application of SC-FDE technique in single-input single-output (SISO) PLC systems in [8]. In this paper, we applied SC-FDE with decision feedback equalizer (DFE) to indoor PLC systems and compared the results with conventional time-domain DFE and OFDM for different impulsive noise levels. Except this work, SC-FDE with linear equalizer is also employed in SISO-PLC channels in [9]-[10]. To the best of our knowledge, no previous work has been reported for employing SC-FDE technique in multi-input multi-output (MIMO) PLC channels, in order to exploit

both diversity and FDE advantages.

In this paper, to employ SC-FDE combined with orthogonal STBCs in PLC channels, we first generalize the Al-Dhahir work to all OSTBCs in which the elements of time-slots are members of the set  $\{0, \pm x_1, \pm \bar{x}_1, \dots, \pm x_K, \pm \bar{x}_K\}$  and propose a new technique applicable to all dispersive multipath channels impaired by impulsive noise. We then apply the proposed technique to PLC channels and simulate the BER performance for both indoor and outdoor PLC channel under different noise conditions. We show that a significant improvement in BER performances is achieved when diversity techniques are combined with SC-FDE. We also compare the BER performance of Alamouti code in both SC-FDE and OFDM and show the superiority of SC-FDE scheme.

The remainder of this paper is organized as follows: A brief review of the SC-FDE and STBC techniques and PLC channel configuration are presented in section II. Section III presents our proposed technique for combining SC-FDE with OSTBCs over dispersive multipath channels. Applying this technique to PLC channels and simulation results for both indoor and outdoor PLC channels are presented in section IV. Section V includes the conclusion.

Notation: Bold upper case and bold lower case letters denote matrices and column vectors respectively; unbold lower case letter stand for scalar quantity;  $(\bar{\cdot})$ ,  $(\cdot)^T$  and  $(\cdot)^H$  denote complex conjugate, transpose, and complex conjugate transpose, respectively;  $\mathbf{0}_N$  is a  $N \times N$  zero matrix; and  $diag(x_1, x_2, \dots, x_N)$  stands for diagonal matrix with  $x_1, x_2, \dots, x_N$  on its diagonal entries.

## II. PRELIMINARY

In this section, we first briefly explain the principal of SC-FDE and STBC techniques and then present the PLC channel and noise models.

### A. SC-FDE System Model

Fig. 1 shows a simplified block diagram of a SC-FDE system with linear equalizer. In the transmitter side, the uncorrelated zero-mean symbols with variance  $\sigma_s^2$  are divided into blocks of  $N$  symbols and each block is prepended with a  $L$ -length CP, where  $L$  is the maximum length of the channel impulse response. Finally, the  $N+L$  length blocks are transmitted through multipath channel. Note that, transmitting CP with each block turn out the linear convolution between transmitted block and channel vector to circulant convolution, and eliminate interblock interference (IBI) by discarding the CP at the receiver side [6]-[7].

At the receiver, the CP is removed and the received block after discarding CP is expressed as:

$$\mathbf{y} = \mathbf{H}\mathbf{x} + \mathbf{n} \quad (1)$$

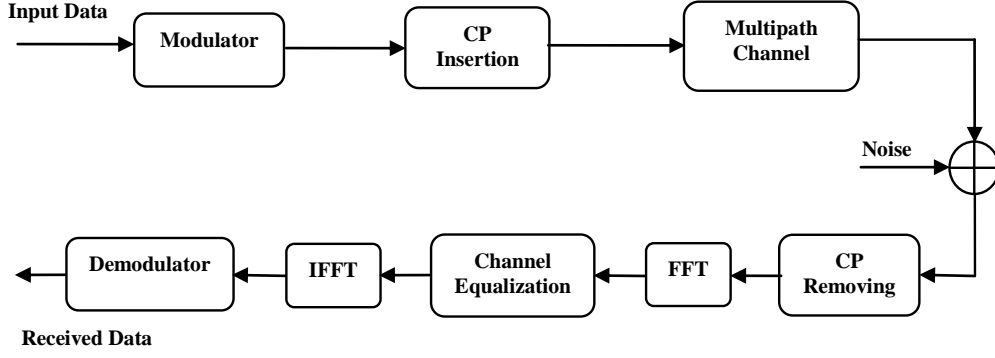


Fig. 1. SC-FDE system with linear equalizer

where  $\mathbf{y}$ ,  $\mathbf{x}$  and  $\mathbf{n}$  are  $N \times 1$  received, input and noise blocks respectively.  $\mathbf{H}$  is the  $N \times N$  channel circulant matrix and can be decomposed as  $\mathbf{H} = \mathbf{F}^* \mathbf{A} \mathbf{F}$ . Where  $\mathbf{F}$  and  $\mathbf{F}^*$  are the  $N \times N$  FFT and IFFT matrixes respectively.  $\mathbf{A}$  is an  $N \times N$  diagonal matrix and its  $(n, n)^{th}$  element is the  $n^{th}$  DFT coefficient of channel impulsive response  $\mathbf{h} = [h(1), \dots, h(L)]^T$ .

Therefore, the frequency domain output of FFT block is as:

$$\mathbf{r} = \mathbf{A} \mathbf{z} + \mathbf{v} \quad (2)$$

where  $\mathbf{r} = \mathbf{F} \mathbf{y}$ ,  $\mathbf{z} = \mathbf{F} \mathbf{x}$  and  $\mathbf{v} = \mathbf{F} \mathbf{n}$ .

The frequency domain linear equalizers based minimum mean square error (MMSE) criteria can be expressed by a  $N \times 1$  vector  $\mathbf{w}$ , whose elements  $w_{MMSE}(n, 1)$  are equal to:

$$w_{MMSE}(n, 1) = \frac{A^*(n, n)}{|A(n, n)|^2 + \frac{1}{SNR}} \quad n = 1, \dots, N \quad (3)$$

where  $SNR = \sigma_s^2 / \sigma_n^2$ ,  $\sigma_s^2$  and  $\sigma_n^2$  are the average power of the transmitted symbols and noise samples respectively. Finally, the equalizer output is converted to time domain by IFFT operation and detection is made based on hard decision by a slicer.

### B. A Brief Review of STBC

STBC technique was originally designed for transmitting multiple copies of a data stream across multiple antennas in frequency-flat fading channels. In general, a STBC is presented by a  $P \times n_t$  matrix  $\mathbf{C}(x_1, x_2, \dots, x_K)$  transmitting  $K$  complex symbols  $x_1, x_2, \dots, x_K$  during  $P$  time-slot intervals (STBC delay) from  $n_t$  antennas with a spatial rate defined as  $R = K/P$ . Note that each row of STBC matrix is a time-slot.

OSTBC is one of the most attractive STBC schemes since due to its orthogonality, a full diversity gain and maximum-likelihood decoding by searching single symbols can be achieved. Orthogonal STBC design was first proposed by Alamouti [11] for 2 transmit antennas and then generalized to more by Tarokh, Jafarkhani and Calderbank [12]. They showed that for complex constellations, when the number of transmit antennas exceeds 2, the code rate is less than unity. For higher number of antennas, they proposed a design method with a code rate equal to 1/2. However, this method is not rate and delay optimal. For example, their proposed code for 3 and 4 transmit antennas results in delay  $P = 8$ . As an alternative, Tirkkonen and Hottinen [13] proposed a 3/4 rate code for three transmit antennas with delay  $P = 4$ .

### C. PLC Channel Configuration

Remarkable attempts have been devoted by researchers to characterize the power line channel and several modeling approaches have been presented for PLC channel. These approaches can be categorized into two general classes: the first is based on the multipath model, proposed by Zimmermann and Dostert [14] and the second is based on the two and multi conductors transmission line theories [15]-[16]. While the former presents the transfer function of the channel with a small set of parameters, the latter needs the whole parameters of the network components. In this paper, we use the multipath approach for channel modeling. Multipath approach is based on the fact that in a wiring network, PLC signals do not propagate along a single path, but suffer from reflections caused by impedance mismatches. In time domain, this model can be described by channel impulsive response as follows:

$$h(t) = \sum_{l=1}^L \beta_l \cdot \delta(t - \tau_l) \quad (4)$$

where  $\beta_l$  and  $\tau_l$  are the amplitude and arrival time of the  $l^{\text{th}}$  multipath component.  $L$  is the number of the propagation paths. However, since the network topology, cable types and connected loads to power networks are not fixed and vary with time and place, this model is not general. To overcome this limitation, open PLC European research alliance (OPERA) presented several reference models for indoor and outdoor PLC channels based on the multipath model [17].

Power-line noises are categorized into two general classes; background and impulsive [18]. Two attractive and popular models for PLC noise are Bernoulli-Gaussian [19] and Middleton class A [20]-[21]. The noise samples for these models are presented by (5) and (6) respectively:

$$n(m) = w(m) + b(m)g_1(m) \quad (5)$$

$$n(m) = w(m) + \sqrt{P(m)}g_2(m) \quad (6)$$

where  $n(m)$  is PLC noise sample.  $w(m)$  is the background noise and is modeled with a complex AWGN with zero-mean and variance  $\sigma_G^2$ . Impulsive noise in Bernoulli-Gaussian approach is modeled by the product of two independent random sequences  $b(m)$  and  $g_1(m)$ : where  $b(m)$  is a real Bernoulli sequence with the probability of success  $p$ , and  $g_1(m)$  is a complex AWGN with zero-mean and variance  $\sigma_I^2$ . Note that the parameter  $p$  can be considered as the probability of impulse occurrence.  $P(m)$  in (6) is a statically independent Poisson distributed random sequence whose power density function is characterized by the impulsive index  $A$  (mean value of Poisson distribution) and  $g_2(m)$  is a complex AWGN with zero-mean and variance  $\sigma_I^2/A$ . In both cases the random sequences are independent and the impulsive to background power ratio is defined as  $PR = \sigma_I^2 / \sigma_G^2$ .

The existing PLC modems use only one transmitting port and one receiving port between phase and neutral wires. To increase the throughput of PLC channels, it is possible to apply MIMO concept to PLC systems by considering emitting/receiving ports in multi-conductor power lines as transmitting and receiving antennas [22]-[23]. In three wires indoor installations, only two different input ports are available at the transmitter side. For outdoor communications four wires usually exist and hence up to three different transmitting ports are available.

We now combine SC-FDE with OSTBCs for multipath channels in next section. Note that while STBC elements for flat fading channels are symbols, for frequency-selective fading channels these elements are blocks of symbols.

### III. A NEW TECHNIQUE FOR COMBINATION OF SC-FDE AND OSTBC

As mentioned in section I, the technique proposed by Al-Dhahir is not applicable to every OSTBC code. For example, Al-Dhahir technique is not applicable to the code given in (A.2) in Appendix. Therefore, to combine SC-FDE and the OSTBCs in which the elements of time-slots are members of the set  $\{0, \pm x_1, \pm \bar{x}_1, \dots, \pm x_K, \pm \bar{x}_K\}$ , a new design method is needed. We will present this method in this section.

Let the  $P \times n_t$  matrix  $\mathcal{C}(x_1, \dots, x_K)$  denotes a complex OSTBC for a flat fading channel. To combine SC-FDE with this code, we need to extend this symbol-level code to a block-level applicable to frequency-selective fading channels. Consider a MISO configuration with  $n_t$  transmit antennas and assume that the output symbols of modulator are divided into blocks (column vectors) of  $N$  symbols and  $K$  blocks form a group  $\mathbf{x}_1, \dots, \mathbf{x}_K$ . The generated groups are used for forming the block-level STBC. The transceiver structure is presented below.

### A. Transmitter Design

Similar to the diversity technique proposed by Al-Dhahir for Alamouti code, we propose the following procedure for extension of symbol-level STBC  $\mathcal{C}(x_1, \dots, x_K)$  to block-level:

- Each zero is replaced by a  $N \times 1$  zero vector denote by  $\mathbf{0}$ .
- Each complex symbol  $\pm x_i$  is replaced by the block  $\pm \mathbf{x}_i$ .
- Each complex conjugate symbol  $\pm \bar{x}_i$  is replaced by a  $N$ -length vector  $\pm \bar{\mathbf{x}}_i'$  (the complex conjugate of  $\pm \mathbf{x}_i'$ ), where  $\mathbf{x}_i'$  is  $\mathbf{x}_i' = [x_i(0), x_i(N-1), \dots, x_i(1)]^T$  and  $x_i(n)$  is the  $n^{\text{th}}$  symbol in the  $i^{\text{th}}$  block.

The  $n^{\text{th}}$  element of  $\mathbf{x}_i'$  is [7]:

$$x_i'(n) = x_i((-n) \bmod N), \quad n = 0, \dots, N-1 \quad (7)$$

Hence, the discrete Fourier transforms of the blocks  $\mathbf{x}_i$  and  $\mathbf{x}_i'$  are the same. Having generated the block-level OSTBC  $\mathcal{C}(\mathbf{x}_1, \dots, \mathbf{x}_K)$ , its elements are prepended with a  $L$ -length CP to remove IBI and make the MISO subchannels circulant.

### B. Receiver Design

The  $i^{\text{th}}$  received block after discarding CP,  $\mathbf{y}^i$ , is expressed as:

$$\mathbf{y}^i = \sum_{j=1}^{n_t} \mathbf{H}_j^i \mathbf{c}_j^i + \mathbf{n}^i, \quad i = 1, \dots, P \quad (8)$$

where  $\mathbf{H}_j^i$  is the  $N \times N$  channel circulant matrix corresponding to the  $j^{\text{th}}$  transmit antenna in the  $i^{\text{th}}$  transmitted block and  $\mathbf{c}_j^i$  is the element of block-level OSTBC matrix  $\mathcal{C}(\mathbf{x}_1, \dots, \mathbf{x}_K)$  corresponding to the  $i^{\text{th}}$  transmitted block from the  $j^{\text{th}}$  antenna.  $\mathbf{n}^i$  is the  $N \times 1$  noise vector in the  $i^{\text{th}}$  received block where its samples are assumed to be independent and identically distributed (i.i.d) and generated according to the presented models in (3) and (4). The MISO subchannels impulse responses are assumed to be constant over  $P$  consecutive blocks and vary independently. Therefore we have:

$$\mathbf{H}_j^1 = \dots = \mathbf{H}_j^P = \mathbf{H}_j, \quad j = 1, \dots, n_t \quad (9)$$

The  $N \times N$  channel matrix  $\mathbf{H}_j$  is circulant matrix corresponding to  $j^{\text{th}}$  MISO subchannels

$h_j = [h_j(1), \dots, h_j(L)]^T$  and is decomposed like previous section.

To design a MMSE equalizer, the received time-domain blocks  $\mathbf{y}^i$  are converted to frequency-domain using FFT block and then rearranged as  $\mathbf{r}_a = \left[ (\mathbf{r}^1)^T, \dots, (\mathbf{r}^P)^T, (\bar{\mathbf{r}}^1)^T, \dots, (\bar{\mathbf{r}}^P)^T \right]^T$ , where

$\mathbf{r}^i = \mathbf{F} \mathbf{y}^i$  is a  $N \times 1$  vector. This rearrangement overcomes the limitation in Al-Dahir technique and allows us to combine SC-FDE with any OSTBC. Using this rearrangement  $\mathbf{r}_a$  can be rewritten as:

$$\mathbf{r}_a = \mathbf{A}_a \mathbf{z} + \mathbf{v} \quad (10)$$

where  $\mathbf{A}_a$  is a  $2PN \times KN$  complex orthogonal matrix,  $\mathbf{z} = \left[ (\mathbf{z}_1)^T, \dots, (\mathbf{z}_K)^T \right]^T$ , where  $\mathbf{z}_i = \mathbf{F} \mathbf{x}_i$ ,  $\mathbf{v} = \left[ (\mathbf{v}^1)^T, \dots, (\mathbf{v}^p)^T, (\bar{\mathbf{v}}^1)^T, \dots, (\bar{\mathbf{v}}^p)^T \right]^T$ , where  $\mathbf{v}^i = \mathbf{F} \mathbf{n}^i$ . The noise samples of the noise vector  $\mathbf{z}_i$  can be calculated as follows:

$$\begin{aligned} z_{ij} &= \sum_{l=1}^N n_{il} \cdot \exp(-j2\pi(j-1)(l-1)) \\ &\triangleq \sum_{l=1}^N n'_{il} \quad j = 1, 2, \dots, N \end{aligned} \quad (11)$$

where  $z_{ij}$  is the  $j^{\text{th}}$  element of the frequency-domain noise vector  $\mathbf{z}_i$ .  $n_{il}$  is the  $l^{\text{th}}$  entry of the time-domain noise vector  $\mathbf{n}_i$  and  $n'_{il} = n_{il} \cdot \exp(-j2\pi(j-1)(l-1))$ . As we mentioned before, the time-domain noise entries  $n_{il}$  are independent non-Gaussian random variables and have been generated using (5) and (6). Therefore,  $n'_{il}$  samples are also independent. As can be seen from (11), the frequency-domain noise sample  $z_{ij}$  is sum of the  $N$  independent non-Gaussian random variables  $n'_{il}$ . For sufficiently large  $N$ , from central limit theorem, the noise sample  $z_{ij}$  can be considered as a zero-mean Gaussian random variable [24]. Gaussian approximation for noise samples at the output of the FFT block is also used in [25]-[26]. In addition, the FFT operation will maintain the i.i.d. property of the noise samples and does not change the variances of the noise samples. Hence in this work, the frequency-domain noise samples  $z_{ij}$  have been considered as i.i.d. zero-mean Gaussian random variables with variance  $\sigma_n^2$ , where  $\sigma_n^2$  is the variance of the time-domain samples  $n_{il}$ .

Multiplying both sides of (10) by the orthogonal matrix  $\mathbf{A}_a^*$  yields:

$$\tilde{\mathbf{r}} = \mathbf{A}_a^* \mathbf{r}_a = \mathbf{A}_c \mathbf{z} + \tilde{\mathbf{v}} \quad (12)$$

where  $\tilde{\mathbf{r}}$  and  $\tilde{\mathbf{v}} = \mathbf{A}_a^* \mathbf{v}$  are  $KN \times 1$  vectors. It is worth saying that the orthogonal transformation  $\mathbf{A}_a^*$  will maintain the i.i.d. and Gaussian properties of the noise samples. Hence, the elements of the vector  $\tilde{\mathbf{v}}$  are i.i.d. zero-mean Gaussian random variables with auto-correlation matrix equal to  $\mathbf{C}_{\tilde{\mathbf{v}}} = \sigma_n^2 \mathbf{A}_c$ , where  $\mathbf{A}_c$  is a  $KN \times KN$  diagonal matrix equal to  $\mathbf{A}_c = \mathbf{A}_a^* \mathbf{A}_a = \text{diag}(\tilde{\mathbf{A}}_1, \dots, \tilde{\mathbf{A}}_K)$ . The diagonal element  $\tilde{\mathbf{A}}_k$  is a  $N \times N$  diagonal matrix given by  $\tilde{\mathbf{A}}_k = \sum_{j=1}^{n_k} d_{kj} |\mathbf{A}_j|^2$  for  $i = 1, 2, \dots, K$ , in which  $d_{kj}$  is a

positive integer. Note that, the value of  $\tilde{\Lambda}_k$  guarantees the full transmitter diversity gain of the proposed technique. We rewrite (12) as follows:

$$\tilde{\mathbf{r}}^k = \tilde{\Lambda}_k \mathbf{z}_k + \tilde{\mathbf{v}}_k, \quad k = 1, 2, \dots, K \quad (13)$$

where the  $N \times 1$  noise vector  $\tilde{\mathbf{v}}_k$  can be calculated from  $\tilde{\mathbf{v}}$  using  $\tilde{\mathbf{v}}_k = \tilde{\mathbf{v}}((k-1)N+1:kN)$  for  $k=1, 2, \dots, K$ , and its samples are i.i.d. zero-mean Gaussian random variables with auto-correlation matrix equal to  $C_{\tilde{\mathbf{v}}_k} = \sigma_n^2 \tilde{\Lambda}_k$ . Therefore, the frequency-domain MMSE equalizer for block  $\tilde{\mathbf{r}}^k$ , denoted by  $\mathbf{w}_k$ , can now be expressed as:

$$w_k(n, 1) = \frac{1}{\tilde{\Lambda}_k(n, n) + \frac{1}{SNR}}, \quad n = 1, \dots, N \quad (14)$$

Finally, the equalizer output is converted to time-domain using IFFT block and the output is applied to a slicer for block detection.

As an example, our proposed technique is applied to 3/4 rate OSTBC presented in (A.2) in Appendix. Note that for this code, such a design is not possible by Al-Dhahir technique. The design details are presented in Appendix and the simulation results for this example are presented in next section.

#### IV. SIMULATION RESULTS

In this section, we present our simulation results for different indoor and outdoor OPERA channels and different noise scenarios using SC transmission, OSTBC and FDE. Since for indoor and outdoor low voltage PLC systems up to three independent feeding ports are available, we present the simulation results for OSTBCs with two and three transmit antennas in this section.

We use the MIMO-PLC model based on the procedure proposed by Canova, Benvenuto and Bisaglia [27]. Actually, this model is an extension of OPERA reference channels to MIMO case. For realization of each subchannel, the taps of SISO-OPERA channel are multiplied by a different random phase  $e^{-j\theta}$  where  $\theta$  is uniformly distributed between the interval  $[0 \ 2\pi]$ . The noise in each MIMO subchannel is also generated based on the models presented in (5) and (6). In these simulations 8-PSK modulation is employed and for a fair comparison, equal radiated powers for MIMO, MISO and SISO configurations are assumed.

##### A. Simulation Results for Indoor PLC

Simulation results for indoor PLC using OPERA indoor reference channels are presented. The results are for a 3-wires indoor PLC structure using Alamouti code .

In Figs. 2 and 3 the simulation results are presented for OPERA channel 1 and 2 respectively. Bernoulli-Gaussian noise with  $p=0.1$  and  $PR=10$  for Fig. 2 and Middleton class A noises with

impulsive index  $A=0.1$  and  $PR=10$  for Fig. 3 is considered. Each Fig. presents the results for SISO,  $2\times 1$  MISO,  $2\times 2$  and MIMO configurations. The superiority of MIMO over MISO, and MISO over SISO are apparent from these results for indoor PLC channels when diversity techniques are combined with SC-FDE under different noise and channel conditions. For example, as can be seen from Fig. 2, at the BER of  $10^{-3}$ , about 15dB SNR gain is achieved for  $2\times 2$  MIMO as compared with SISO and this gain is about 10dB in Fig. 3. Note that the superiority of MISO over SISO is due to full transmitter diversity gain of MISO scheme and the superiority of MIMO over MISO is due to the fact that both transmitter and receiver diversities are employed in MIMO.

To verify our simulations, the performances of OPERA channels 1 and 4 are compared in Fig. 4 for identical noise conditions. The performance of OPERA channel 3 under Bernoulli-Gaussian noise for different Bernoulli parameters ( $p$ ) and different impulsive to background power ratios ( $PR$ ) are also compared in Figs. 5 and 6 respectively. The results in Figs. 5 and 6 are also compared with the situation where the channel is only affected by AWGN noise. Simulation results for SISO and  $2\times 2$  MIMO are shown in Figs. 4 - 6. As expected the system performance improves for a better channel and noise circumstances. In addition, the advantages of diversity in indoor PLC channels are apparent from figs 4 to 6. For example, Fig. 4 shows about 10dB SNR gain at the BER of  $10^{-3}$  for channel 4. The performance degradation of impulsive noise is also apparent from Figs. 5 and 6 when the impulsive noise curves are compared with the AWGN noise curves.

Space-time and space-frequency block codes have been proposed for MIMO-OFDM systems by many research works like [28]-[30]. Here, to compare our block-level STBC SC-FDE technique with OFDM, we use the block-level STBC-OFDM technique for Alamouti code presented by Liu et al. [28]. It is worth saying that in this paper, a proper design for combination of Alamouti code with OFDM for frequency-selective wireless channels is presented. The comparison of our technique with the OFDM are presented in Fig. 7 for OPERA channel 4 under Middleton class A noise with  $A=0.25$  and  $PR=40$ . This simulation is performed for SISO and  $2\times 2$  MIMO configurations. As can be seen, the two systems behave similar at low and medium SNRs, while at high SNRs SC-FDE performs better than OFDM. It is worth saying that while the complexity of SC-FDE is not more than OFDM; it does not suffer from the OFDM drawbacks like high peak to average power ratio and carrier frequency offset sensitivity.

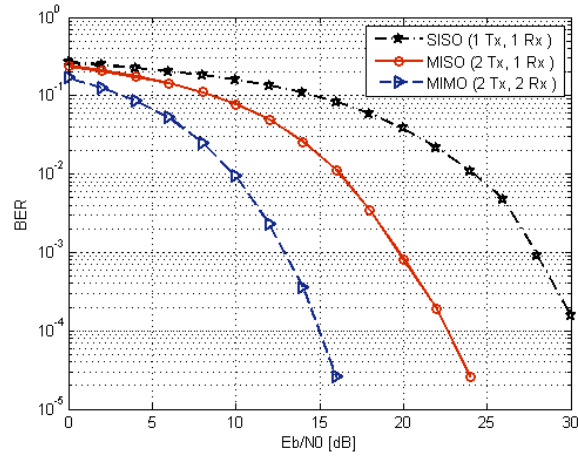


Fig. 2. BER performance of OPERA indoor reference channel 1 under Bernoulli- Gaussian noise with  $p = 0.1$  and  $PR = 10$ .

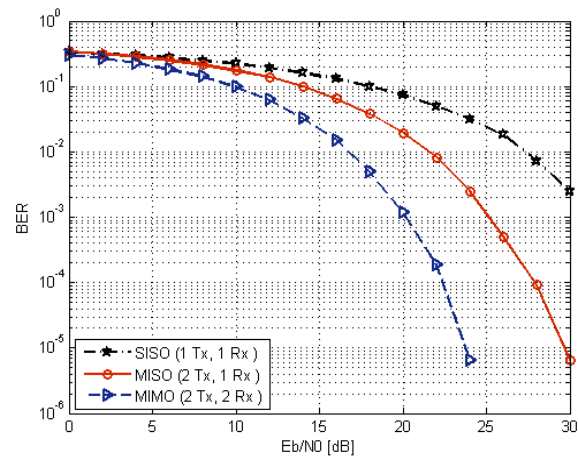


Fig. 3. BER performance of OPERA indoor reference channel 2 under Middleton class A noise with  $A = 0.1$  and  $PR = 10$ .

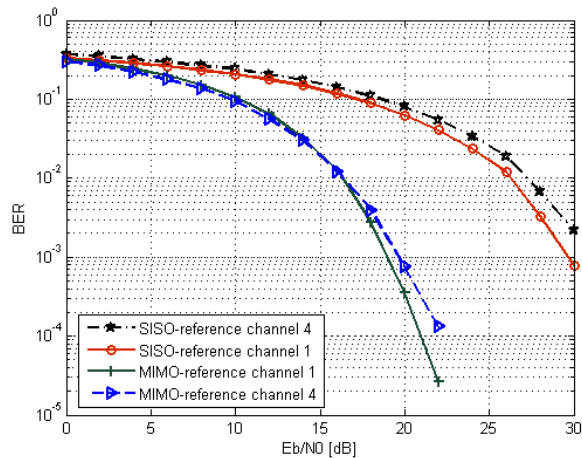


Fig. 4. BER performance of OPERA indoor reference channel 1 and 4 under Bernoulli-Gaussian noise for SISO and 2x2 MIMO configurations.

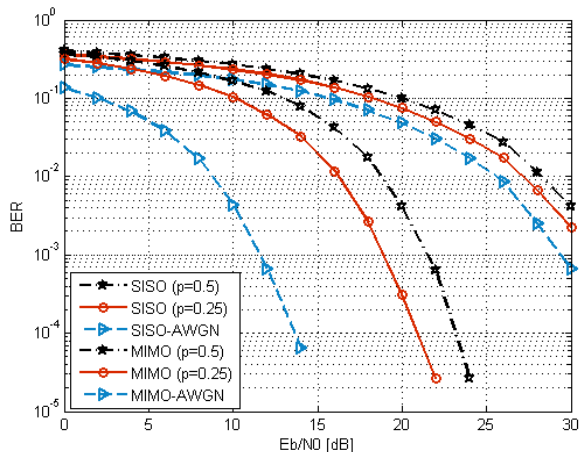


Fig. 5. BER performance of OPERA indoor reference channel 3 under Bernoulli-Gaussian noise with different  $p$ .

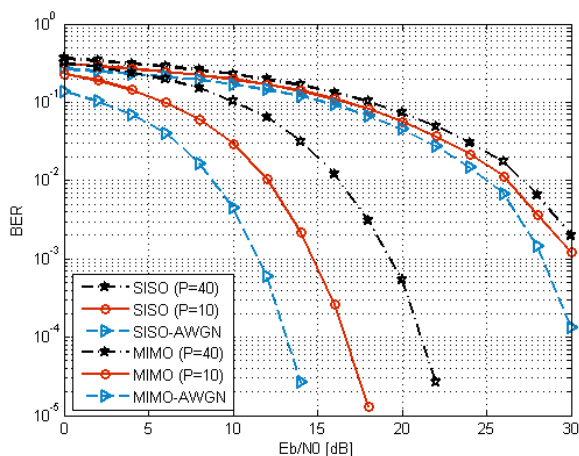


Fig. 6. BER performance of OPERA indoor reference channel 3 under Bernoulli-Gaussian noise with different  $PR$ .

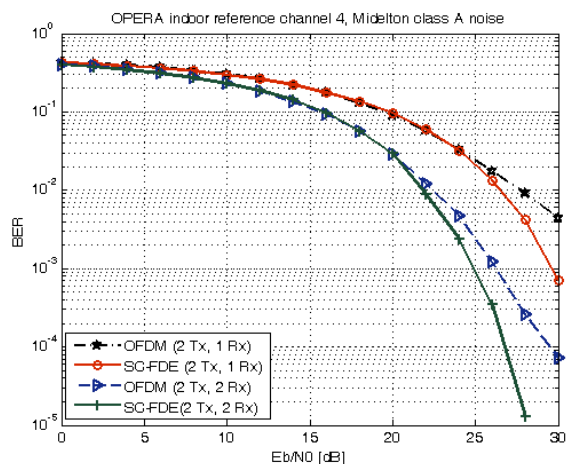


Fig. 7. BER performances of OFDM and SC-FDE systems using Alamouti code and OPERA reference channel 4.

### B. Simulation Results for Outdoor PLC

Since usually 4 wires are available in outdoor low voltage power networks, we can use up to 3 transmitting channels for PLC purposes. For outdoor, OSTBCs presented in (A.1) and (A.2) for two different code rates (1/2 and 3/4) together with SC-FDE technique are employed. Similar to indoor,

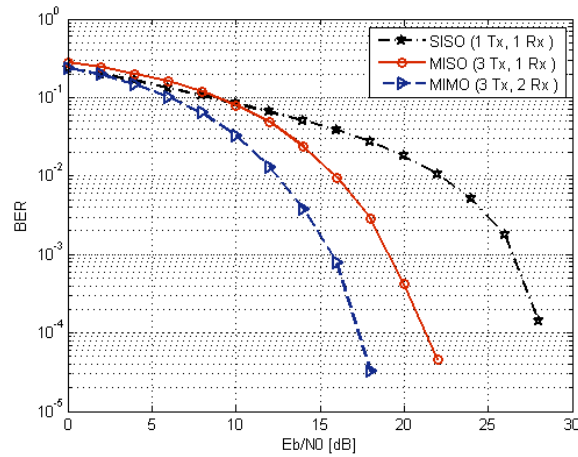


Fig. 8. BER performance of OPERA outdoor channel 1 using half rate code under Bernoulli- Gaussian noise with  $\rho = 0.25$  and  $PR = 40$ .

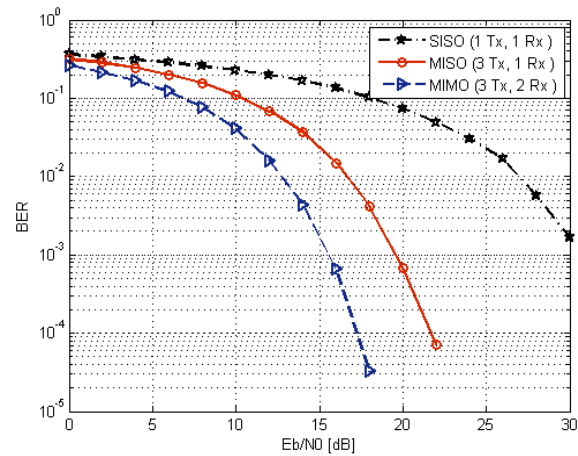


Fig. 9. BER performance of OPERA outdoor channel 2 using half rate code under Bernoulli- Gaussian noise with  $\rho = 0.25$  and  $PR = 40$ .

we use OPERA reference channels presented for outdoor wires [15]. Our simulations results are presented for SISO,  $3 \times 1$  MISO and  $3 \times 2$  MIMO configurations.

Figs. 8 and 9 present the simulation results for outdoor OPERA channel models 1 and 2 respectively using half rate OSTBC given in the Appendix. The noise samples for both cases are generated by Bernoulli-Gaussian model with  $\rho = 0.25$  and  $PR = 40$ . As can be seen from these results, a significant improvement is achieved when OSTBC combined with SC-FDE in outdoor PLC channels. For example, in Fig. 9 at the BER of  $10^{-3}$  about 15dB SNR gain is achieved in  $3 \times 2$  MIMO as compared with SISO.

Figs. 10 and 11 show the simulation results for OPERA outdoor reference channels 5 and 6 using  $3/4$  rate OSTBC given in (A.2) under Middleton class A noise. The Middleton class A noise parameters for both channels are  $A = 0.1$  and  $PR = 40$ . Similar to half rate code, the advantage of diversity techniques combined with SC-FDE is apparent from these Figs for this case. For example, in Fig. 10 at the BER of  $10^{-3}$  about 10dB SNR gain is achieved in  $3 \times 2$  MIMO as compared with SISO.

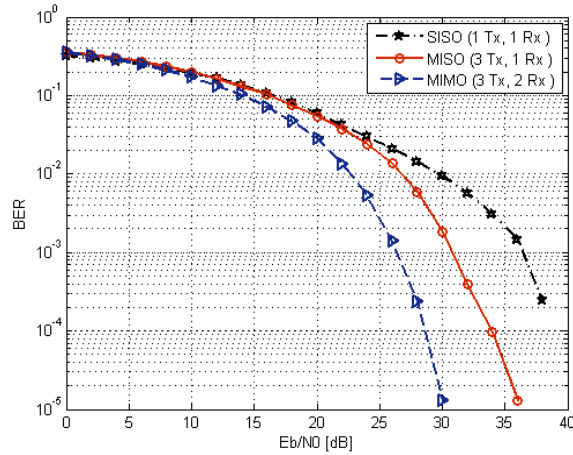


Fig. 10. BER performance of OPERA outdoor reference channel 5 using 3/4 rate code under Middleton class A noise with  $A = 0.1$  and  $PR = 40$ .

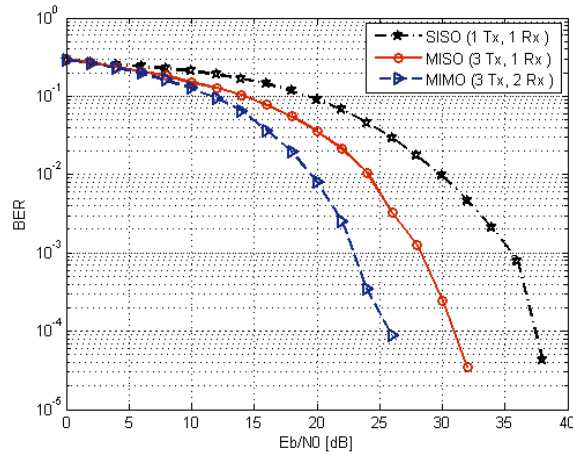


Fig. 11. BER performance of OPERA outdoor reference channel 6 using 3/4 rate code under Middleton class A noise with  $A = 0.1$  and  $PR = 40$ .

## V. CONCLUSION

In this paper a new approach for broadband MIMO-PLC transmission over both indoor and outdoor low voltage power lines using SC-FDE technique combined with OSTBC was presented. A new technique for combination of SC-FDE with orthogonal STBCs applicable to all dispersive multipath channels impaired by impulsive noise is presented. The proposed technique is then applied to space diversity frequency-selective PLC channels. Simulation results were presented for different indoor and outdoor channels under different noise scenarios. Simulation results show that using the proposed diversity technique results in a significant improvement in BER performance as compared with SISO under all channel and noise scenarios. The superiority of our proposed technique over OFDM, especially at high SNRs, was also demonstrated.

## APPENDIX

Here we first introduce OSTBCs required in this paper and then present the design method for

combining SC-FDE with 3/4 rate code.

The 1/2 and 3/4 rate orthogonal codes for 4 antennas given in [12] and [13] are respectively:

$$\mathbf{C}(x_1, \dots, x_4) = \begin{bmatrix} x_1 & x_2 & x_3 & x_4 \\ -x_2 & x_1 & -x_4 & x_3 \\ -x_3 & x_4 & x_1 & -x_2 \\ -x_4 & -x_3 & x_2 & x_1 \\ \bar{x}_1 & \bar{x}_2 & \bar{x}_3 & \bar{x}_4 \\ -\bar{x}_2 & \bar{x}_1 & -\bar{x}_4 & \bar{x}_3 \\ -\bar{x}_3 & \bar{x}_4 & \bar{x}_1 & -\bar{x}_2 \\ -\bar{x}_4 & -\bar{x}_3 & \bar{x}_2 & \bar{x}_1 \end{bmatrix} \quad (\text{A.1})$$

$$\mathbf{C}(x_1, \dots, x_3) = \begin{bmatrix} x_1 & x_2 & x_3 & 0 \\ -\bar{x}_2 & \bar{x}_1 & 0 & -x_3 \\ -\bar{x}_3 & 0 & \bar{x}_1 & x_2 \\ 0 & \bar{x}_3 & -\bar{x}_2 & x_1 \end{bmatrix} \quad (\text{A.2})$$

The OSTB codes for 3 transmit antennas can be obtained by removing the 4<sup>th</sup> column of the above codes .

To combine the SC-FDE with 3/4 rate code presented in (A.2), we extend the code to block level based on the proposed prouder given in section III. This leads to:

$$\mathbf{C}(x_1, x_2, x_3) = \begin{bmatrix} x_1 & x_2 & x_3 & 0 \\ -\bar{x}'_2 & \bar{x}'_1 & 0 & -x_3 \\ -\bar{x}'_3 & 0 & \bar{x}'_1 & x_2 \\ 0 & \bar{x}'_3 & -\bar{x}'_2 & x_1 \end{bmatrix} \quad (\text{A.3})$$

CP is prepended to this extended code before transmission. The received blocks after removing CP and passing through the FFT block are rearrange as:

$$\mathbf{r}_a = \begin{bmatrix} \mathbf{r}^1 \\ \mathbf{r}^2 \\ \mathbf{r}^3 \\ \mathbf{r}^4 \\ \bar{\mathbf{r}}^1 \\ \bar{\mathbf{r}}^2 \\ \bar{\mathbf{r}}^3 \\ \bar{\mathbf{r}}^4 \end{bmatrix} = \begin{bmatrix} \mathbf{A}_1 & \mathbf{A}_2 & \mathbf{A}_3 \\ \mathbf{0}_N & \mathbf{0}_N & -\mathbf{A}_4 \\ \mathbf{0}_N & \mathbf{A}_4 & \mathbf{0}_N \\ \mathbf{A}_4 & \mathbf{0}_N & \mathbf{0}_N \\ \mathbf{0}_N & \mathbf{0}_N & \mathbf{0}_N \\ -\mathbf{A}_2^* & \mathbf{A}_1^* & \mathbf{0}_N \\ \mathbf{A}_3^* & \mathbf{0}_N & -\mathbf{A}_1^* \\ \mathbf{0}_N & -\mathbf{A}_3^* & \mathbf{A}_2^* \end{bmatrix} \begin{bmatrix} \mathbf{z}_1 \\ \mathbf{z}_2 \\ \mathbf{z}_3 \end{bmatrix} + \begin{bmatrix} \mathbf{v}^1 \\ \mathbf{v}^2 \\ \mathbf{v}^3 \\ \mathbf{v}^4 \\ \bar{\mathbf{v}}^1 \\ \bar{\mathbf{v}}^2 \\ \bar{\mathbf{v}}^3 \\ \bar{\mathbf{v}}^4 \end{bmatrix} = \mathbf{A}_a \mathbf{z} + \mathbf{v} \quad (\text{A.4})$$

where  $\mathbf{A}_a$  is a  $8N \times 3N$  complex orthogonal matrix. Multiplying both side of (A.4) by  $\mathbf{A}_a^*$  yeilds:

$$\tilde{\mathbf{r}}_a = \begin{bmatrix} \tilde{\mathbf{r}}^1 \\ \tilde{\mathbf{r}}^2 \\ \tilde{\mathbf{r}}^3 \end{bmatrix} = \begin{bmatrix} \tilde{\Lambda}_1 & \mathbf{0}_N & \mathbf{0}_N \\ \mathbf{0}_N & \tilde{\Lambda}_2 & \mathbf{0}_N \\ \mathbf{0}_N & \mathbf{0}_N & \tilde{\Lambda}_3 \end{bmatrix} \begin{bmatrix} \mathbf{z}_1 \\ \mathbf{z}_2 \\ \mathbf{z}_3 \end{bmatrix} + \begin{bmatrix} \tilde{\mathbf{v}}^1 \\ \tilde{\mathbf{v}}^2 \\ \tilde{\mathbf{v}}^3 \end{bmatrix} \quad (\text{A.5})$$

Finally, the frequency-domain equalizer taps can be easily found from (14) for

$\tilde{\Lambda}_1 = \tilde{\Lambda}_2 = \tilde{\Lambda}_3 = \sum_{j=1}^4 |A_j|^2$ . Obviously for three transmit antennas it is enough to remove the 4<sup>th</sup> column of the (A.3) and substitute  $A_4$  with the zero matrix  $\mathbf{0}_N$  in (A.4) and (A.5).

#### ACKNOWLEDGMENT

This work is supported in part by Iran Telecommunication Research Center (ITRC).

#### REFERENCES

- [1] S. Galli, A. Scaglione and Z. Wang, "For the Grid and Through the Grid: The Role of Power Line Communications in the Smart Grid," *Proceedings of the IEEE - Special Issue on Smart Grid*, vol. 99, no. 6, pp. 998-1027, June 2011.
- [2] K.-H. Kim, et al., "Capacity analysis of relay channels for medium voltage powerline access network," *IEE International Conference in Computing, Networking and Communications (ICNC)*, pp. 917 – 921, Jan. 30 -Feb. 2, 2012.
- [3] E. Biglieri, "Coding and Modulation for a Horrible Channel," *IEEE Commun. Mag.*, vol. 41, no. 5, pp. 92-98, May, 2003.
- [4] D. Falconer, S. L. Ariyavisitakul, A. Benyamin-Seeyar and B. Eidson, "Frequency domain equalization for single-carrier broadband wireless systems," *IEEE Commun. Mag.*, vol. 40, no. 4, pp. 58-66, Apr. 2002.
- [5] F. Pancaldi, et al., "Single-Carrier Frequency domain Equalization," *IEEE Signal Processing Mag.*, vol. 25, no. 5, pp. 37-56, Sep. 2008.
- [6] H. Sari, G. Karam, and I. Jeanclaude, "Transmission techniques for digital terrestrial TV broadcasting," *IEEE Commun. Mag.*, vol. 33, no. 2, pp. 100–109, Feb. 1995.
- [7] N. Al-Dhahir, "Single-carrier frequency-domain equalization for space-time block-coded transmissions over frequency-selective fading channels," *IEEE Commun. Lett.*, vol. 5, no. 7, pp. 304–306, July 2001.
- [8] Mohsen Sheikh-Hosseini, and Mohammad Molavi., "Single Carrier Transmission in Power Line Channels Using Time and Frequency Domain Decision Feedback Equalizations," *Int. J. Tomogr. Stat.*, vol. 12, no. F09, pp. 94-104, Fall 2009.
- [9] F. A. La-Gatta, A. P. Legg and R. Machado, "Coded CP-SC Communication Scheme for Outdoor Power Line Communications," in *Proc. IEEE International Symposium on Power line Communications and Its Applications (ISPLC)*, Rio de Janeiro, Brazil, pp. 28-31, March 2010.
- [10] Y. H. Ng, and T. Ch. Chuah, "Single-Carrier Cyclic Prefix-Assisted PLC systems with Frequency-Domain Equalization for High-Data-Rate Transmission," *IEEE Power Del.*, vol. 25, no. 3, pp. 1450-1457, July 2010.
- [11] S. Alamouti, "A Simple Transmitter Diversity Scheme for Wireless Communications," *IEEE J. Select. Areas Commun.*, vol. 16, no. 8, pp. 1451–1458, Aug. 1998.
- [12] V. Tarokh, H. Jafarkhani and A. R. Calderbank, "Space Time Block Codes from Orthogonal Design," *IEEE Trans. Inform. Theory*, vol. 45, no. 5, pp. 1456- 1466, July 1999.
- [13] O. Tirkkonen and A. Hottinen, "Square-matrix embeddable space-time block codes for complex signal constellations," *IEEE Trans. Inform. Theory*, vol. 48, no. 2, pp. 384 – 395, Feb. 2002.

- [14] M. Zimmermann and K. Dostert, "A Multipath Model for the Powerline Channel", *IEEE Trans. Commun.*, vol 50, no. 4, pp. 553-559, Apr. 2002.
- [15] H. Meng, Y. L. Guan, C. L. Law, P. L. So, E. Gunawan, and T. Lie, "Modeling of Transfer Characteristics for the Broadband Power Line Communication Channel," *IEEE Trans. Power Del.*, vol. 19, no. 3, pp. 1057–1064, Jul. 2004.
- [16] S. Galli and T. Banwell, "A deterministic frequency-domain model for the indoor power line transfer function", *IEEE J. Sel. Areas Commun.*, vol. 24, no. 7, pp. 1304–1316, Jul. 2006.
- [17] M. Babic, M. Hagenau, K. Dostert and J. Bausch, "Theoretical postulation of PLC channel model", *Tech. Rep., Open PLC European Research Alliance (OPERA)*, March 2005.
- [18] M. Zimmermann, and K. Dostert, "Analysis and modeling of impulsive noise in broad-band powerline communications," *IEEE Trans. Electromagn. Compat.*, Feb. 2002.
- [19] M. Ghosh, "Analysis of the effect of impulsive noise on multicarrier and single carrier QAM systems," *IEEE Trans. Commun.*, vol. 44, pp. 145-147, Feb.1996.
- [20] D. Middleton, "Statistical-physical model of electromagnetic interference," *IEEE Trans. Electromagn. Compat.*, vol. EMC-19, no. 3, pp. 106–126, Aug. 1977.
- [21] G. Pay and M. Safak, "Performance of DMT Systems under Impulsive Noise," in Proc. IEEE International Symposium on Power line Communications and Its Applications (ISPLC), Sweden, pp. 109-114, Apr. 2001.
- [22] L. Stadelmeier, et al. , "MIMO for inhome power line communications," In Proceeding of International Conference on Source and Channel Coding (SCC) 2008; Ulm, Germany, Jan. 2008.
- [23] T. Sartenaer and P. Delogne, "Powerline Cables Modeling for Broadband Communications," In Proceeding of International Symposium on Power line Communication and its Applications, Sweden, pp. 331-337, Apr. 2001.
- [24] A. Papoulis, "Probability, random variables and stochastic processes," *McGraw-Hill Book*, 1984.
- [25] Y. H. Ma, P.L.So, and E. Gunawan, "Performance analysis of OFDM systems for broadband power line communications under impulsive noise and multipath effects," *IEEE Transaction on Power Delivery*, vol. 20, pp. 674–682, April 2005.
- [26] S. M. Navidpour, P. Amirshahi, M. Kavehrad, "Performance Analysis of Coded MC-CDMA in Powerline Communication Channel with Implusive Noise," IEEE International Symposium on Power Line Communications (ISPLC'06), Orlando, USA, pp. 267-272, March 2006.
- [27] A. Canova, N. Benvenuto and P. Bisaglia, "Receivers for MIMO-PLC channels: Throughput Comparison," in Proc. IEEE International Symposium on Power line Communications and Its Applications (ISPLC), Rio de Janeiro, Brazil, pp. 114-119 March 2010.
- [28] Z. Liu, G. B. Giannakis, B. Muquet and S. Zhou, "Space-Time Coding for Broadband Wireless Communications," *Wireless Syst. Mobile Comput.*, vol. 1, pp. 35-53, 2001.
- [29] Andreas F. Molisch, Moe Z. Win, and Jack H. Winters, "Space-Time-Frequency (STF) Coding for MIMO-OFDM Systems," *IEEE Communications Letters*, vol. 6, no. 9, pp. 370-372, Sept. 2002.
- [30] H. Boelcskei, M. Borgmann, and A. Paulraj, "Impact of the propagation environment on the performance of space-frequency coded MIMO-OFDM" *IEEE J. Sel. Areas Commun.*, vol. 21, no. 3, pp. 427–439, Apr. 2003.